INTERNATIONAL JOURNAL OF ROBUST AND NONLINEAR CONTROL
Int. J. Robust. Nonlinear Control 2013; **23**:104–122
Published online 9 October 2011 in Wiley Online Library (wileyonlinelibrary.com). DOI: 10.1002/rnc.1823

Robust control of robot manipulators based on uncertainty and disturbance estimation

Jaywant P. Kolhe, Md Shaheed, T. S. Chandar and S. E. Talole*,†

Department of Aerospace Engineering, Defence Institute of Advanced Technology, Girinagar, Pune 411025, India

SUMMARY

In this work, uncertainty and disturbance estimation (UDE) based robust trajectory tracking controller for rigid link manipulators was proposed. The UDE was employed to estimate the composite uncertainty that comprises the effects of system nonlinearities, external disturbances, and parametric uncertainties. A feedback linearization based controller was designed for trajectory tracking, and the same was augmented by the UDE-estimated uncertainties to achieve robustness. The resulting controller however required measurement of joint velocities apart from the joint positions. To address the issue, an observer that employed the UDE-estimated uncertainties for robustness was proposed, giving rise to the UDE-based controller–observer structure. Closed-loop stability of the overall system was established. The notable feature of the proposed design was that it neither required accurate plant model nor any information about the uncertainty. Also, the design needed only joint position measurements for its implementation. To demonstrate the effectiveness, simulation results of the proposed approach as applied to the trajectory tracking control of two-link robotic manipulator and comparison of its performance with some of the well-known existing controllers were presented. Lastly, hardware implementation of the proposed design for trajectory control of Quanser's single-link flexible joint module was carried out, and it was shown that the proposed strategy offered a viable approach for designing implementable robust controllers for robots.

Received 27 November 2010; Revised 21 March 2011; Accepted 4 September 2011

KEY WORDS: uncertainty and disturbance estimation; feedback linearization; robot manipulator; robust control; robust observer; controller–observer structure

1. INTRODUCTION

Control of robotic manipulators is an area of active research, and, owing to its highly coupled nonlinear dynamics, it offers a challenging task for high performance control system design. The task gets further compounded when the system is subjected to various model uncertainties and unmeasurable external disturbances. As the model-based control strategies such as the one based on feedback linearization (FL) approach [1] may not offer satisfactory performance in the presence of uncertainties, various robust control approaches have been presented in the literature for designing tracking controllers for robot manipulators. Designs based on Proportional-derivative (PD) control [2], Proportional-integral-derivative [3], H-infinity [4], Lyapunov-based theory [5], variable structure control [6], optimal control [7], state dependent Riccati equation approach [8], neural networks [9], and fuzzy logic [10] are some representative approaches to mention, and an exhaustive survey of various strategies proposed for the design of robust controllers for robotic manipulators can be found in [11, 12].

*Correspondence to: S. E. Talole, Department of Aerospace Engineering, Defence Institute of Advanced Technology, Girinagar, Pune 411025, India.
†E-mail: setalole@hotmail.com

In many of the robust control formulations presented in the literature, there exists certain issues that need attention. Firstly, in the number of the proposed controllers, knowledge of some characteristic of uncertainty is assumed. To cite a few examples, in [13], the uncertainty is assumed to be bounded by higher-order polynomials in system states. In [14], the uncertainty is assumed to be bounded by a known continuous function. Similarly, in [15], a finite-time robust control formulation is presented wherein the knowledge of uncertainty bound is needed. Also, as is well known, the formulations based on sliding mode control (SMC) and Lyapunov-based approaches in general require a priori knowledge of bounds of uncertainty. As the uncertainties are generally unknown or poorly known, not having accurate information on the characteristics of the uncertainty results into degraded performance. For example, when the knowledge of bound on uncertainties is not available, the use of highly conservative bound results in excessive control effort, and use of lower bounds may result in degradation of performance or even in instability. Secondly, most of the controllers proposed for robotic manipulators need the measurement of joint positions and velocities. Whereas position can be accurately measured by good precision encoders, velocity measurement is often an issue because of measurement noise [16]. Apart from this, the cost and weight of an additional sensor can also be a deterrent. One approach to address the issue is to obtain the estimate of velocity from position measurement through approximate differentiation. However, the resulting estimate may not be satisfactory. A better alternative is to obtain the velocity states by designing an appropriate observer [17]. However, observers designed based on an assumed system model may suffer from robustness when the model uncertainties show up. Also, as the separation principle is not, in general, valid in nonlinear systems, the closed-loop stability of the controller–observer system remains an issue. Lastly, an important consideration in designing controllers in robotic system is that it should be simple from real-time implementation point of view.

In this paper, an uncertainty and disturbance estimation (UDE) [18] based robust trajectory tracking controller is proposed for rigid link manipulators. An FL-based controller is formulated by considering the system nonlinearities, uncertainties, and external disturbances as a composite uncertainty. The FL controller is then augmented by the UDE-estimated uncertainty [19] to achieve robustness. As the resulting controller requires joint velocities apart from the joint positions, a robust observer is proposed to provide estimate of the joint velocities. The observer design too employs the UDE-estimated uncertainty to achieve robustness, thus giving rise to the UDE-based controller–observer structure. Closed-loop stability of the controller–observer structure is established. The significant feature of the proposed approach is that it does not need any information about the uncertainties. Also, the design does not require accurate plant model and needs measurement of only link positions for its implementation. Effectiveness of the proposed approach is demonstrated through simulations with significant uncertainties in the system model. Next, numerical simulation results are presented by comparing the performance of the proposed approach with some well-known existing designs to highlight the performance benefits of the proposed design. Finally, hardware implementation of the proposed controller for trajectory tracking of Quanser's single-link flexible joint module is carried out, and the related results are presented.

The remaining paper is organized as follows. In Section 2, a mathematical model and FL-based controller design for the two-link robot manipulator is presented. An overview of the UDE approach and its application for robustification of the FL control is the subject of Section 3. In Section 4, the UDE-based controller–observer structure is presented whereas closed-loop stability of the overall system is presented in Section 5. In section 6, simulation results of the application of the proposed strategy are given. The results on comparative study of the proposed design with some well-known existing control strategies are the subject of Section 7. In Section 8, the results of the experimental validation of the proposed design as applied to Quanser's rigid link flexible joint module are presented, and lastly, Section 9 concludes this work.

2. STATEMENT OF THE PROBLEM

2.1. Dynamics of robot manipulator

The dynamics of a two-link rigid robot manipulator, shown in Figure 1, can be obtained via the Euler–Lagrangian formalism as [20]

DOI: 10.1002/rnc

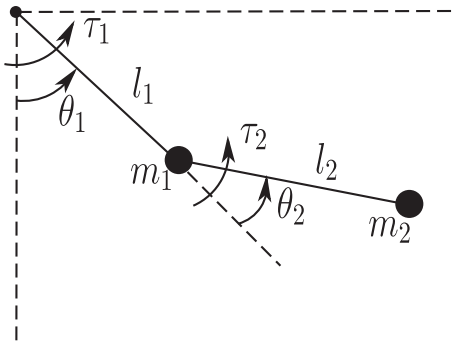

Figure 1. Two link planar robot manipulator.

$$M(\theta)\ddot{\theta} + C(\theta, \dot{\theta}) + K(\theta) = \tau \tag{1}$$

where $\theta = [\theta_1 \ \theta_2]^T$ is the vector of joint positions, $\dot{\theta} = [\dot{\theta}_1 \ \dot{\theta}_2]^T$ is the vector of joint velocities, $M(\theta)$ is the inertia matrix, $C(\theta, \dot{\theta})$ is the centripetal and Coriolis torque matrix, $K(\theta)$ represents the gravitational torques, and $\tau = [\tau_1 \ \tau_2]^T$ represents the input torque vector. For the two-link robotic manipulator, the various matrices appearing in Equation (1) can be obtained as

$$\begin{aligned} M(\theta) &= \begin{bmatrix} m_1 l_1^2 + m_2(l_1^2 + l_2^2 + 2l_1 l_2 \cos\theta_2) & m_2(l_2^2 + l_1 l_2 \cos\theta_2) \\ m_2(l_2^2 + l_1 l_2 \cos\theta_2) & m_2 l_2^2 \end{bmatrix} \\ C(\theta, \dot{\theta}) &= \begin{bmatrix} -m_2 l_1 l_2 \sin\theta_2 \dot{\theta}_2 (2\dot{\theta}_1 + \dot{\theta}_2) \\ m_2 l_1 l_2 \dot{\theta}_1^2 \sin\theta_2 \end{bmatrix} \\ K(\theta) &= \begin{bmatrix} (m_1 + m_2) g l_1 \sin\theta_1 + m_2 g l_2 \sin(\theta_1 + \theta_2) \\ m_2 g l_2 \sin(\theta_1 + \theta_2) \end{bmatrix} \end{aligned} \tag{2}$$

where l_1 and l_2 are the lengths of the links whereas m_1 and m_2 are the masses as shown in Figure 1. The quantity, g, is the gravitational acceleration. The control objective is to design a robust controller using only joint position feedback such that the manipulator joint position vector, $\theta(t)$, tracks the desired joint position $\theta^\star(t)$ as per the specifications imposed.

2.2. *Feedback linearization based control*

The FL [1,21] is one of the most prominent approaches in nonlinear control systems design. One of the advantages offered by the FL approach is that it provides a systematic framework for designing controllers for nonlinear systems. The inverse dynamics or computed torque methods in robotics are essentially the FL controllers. The basic idea underlying the FL is to seek a nonlinear state-coordinate transformation and nonlinear feedback control law under which the system exhibits linear closed-loop relationship. Once the system is linearized, any standard linear technique can be employed for designing the control law to achieve desired performance. To this end, the design consists typically of two steps: firstly, constructing a nonlinear control law as an *inner-loop control* and then designing a second stage or *outer-loop control* to obtain the desired closed-loop performance. In this work, the FL approach is employed for designing the tracking controller for robot manipulator.

Consider the dynamics given by Equation (1). As the inertia matrix of the two-link robot manipulator is non-singular in the whole state-space, the dynamics can be rewritten as

$$\ddot{\theta} = -M(\theta)^{-1} C(\theta, \dot{\theta}) - M(\theta)^{-1} K(\theta) + M(\theta)^{-1} \tau \tag{3}$$

For the system of (3), nonlinear coordinate transformation is not required, and the control, which achieves FL with the link positions as outputs can be obtained as [1]

$$\tau = C(\theta, \dot{\theta}) + K(\theta) + M(\theta)\nu \tag{4}$$

DOI: 10.1002/rnc

where $\nu = [\nu_1 \ \nu_2]^T$ is the outer-loop control. Substituting the FL control (4) in Equation (3) results into a linear and decoupled input–output relationship as

$$\ddot{\theta} = \nu \tag{5}$$

Now, defining the outer-loop control, ν, as

$$\nu_i = \ddot{\theta}_i^\star + k_{i2}(\dot{\theta}_i^\star - \dot{\theta}_i) + k_{i1}(\theta_i^\star - \theta_i), \qquad i = 1, 2 \tag{6}$$

where the starred quantities represent the reference trajectories of the corresponding link positions. Applying Equation (6) to Equation (5) results into the tracking error dynamics as

$$\ddot{e}_{ic} + k_{i2}\dot{e}_{ic} + k_{i1}e_{ic} = 0 \tag{7}$$

where $e_{ic}(t) = \theta_i^\star(t) - \theta_i(t)$ is the position tracking error of the i-th link. The controller gains, k_{ij}, are the design parameters and are needed to be chosen such that desired tracking performance is achieved.

As is well known, the FL control requires exact cancellation of the nonlinearities. It offers asymptotic tracking of the reference trajectory only when the models are known exactly, and the fed back states are measured without any error. In reality, these conditions are hard to meet, and so the FL control law may not offer satisfactory performance. Because modeling uncertainties are almost always present, there is a need to robustify the FL-based controller. Another important consideration in FL-based control law is its implementation. The controller requires knowledge of link velocities apart from the link positions. In view of the reasons stated earlier, it is necessary to address the issue of requirement of link velocities as well.

3. UNCERTAINTY AND DISTURBANCE ESTIMATION BASED CONTROLLER

One approach for designing robust control for uncertain systems is to estimate the effect of uncertainties and disturbances acting on the system and compensate it by augmenting the controller designed for nominal system. Techniques like disturbance observer [22], unknown input observer [23], and perturbation observer [24] have been in place for quite sometime to estimate the effects of uncertainties and disturbances. Application of these techniques for estimating disturbance in robotic manipulators has also appeared [25,26]. A time delay control (TDC) is one such well-known strategy used for estimation of system uncertainties [27]. In TDC, a function representing the effect of uncertainties and external disturbances is estimated directly using information in the recent past, and then a control is designed using this estimate in such a way to cancel out the effect of the unknown dynamics and external disturbances. Application of TDC in robotics has also been reported in the literature [28,29]. Following the line of TDC and addressing some issues associated with it, a novel UDE technique is proposed in [18]. Since then, application of UDE in various contexts has appeared in the literature. An application of the UDE in robustifying a feedback linearizing control law for a robot having joint flexibility is presented in [30] wherein the effect of joint flexibility is treated as a disturbance. An application of UDE in overcoming the issues of requirement of knowledge of uncertainty bound and chattering in SMC can be found in [31]. In [32] and [33], the UDE-based robust control designs for uncertain linear and nonlinear systems with state delays are presented, and the authors have shown that the designs offer excellent tracking and disturbance rejection performance. In [19], an application of the UDE in robustification of the input-output linearization (IOL) controller is presented, wherein the UDE-estimated uncertainties are used in robustifying an IOL controller. The robustification is achieved by estimating the uncertainties and external unmeasurable disturbances using the UDE and compensating the same by augmenting the IOL controller designed for nominal system. In this work, the UDE approach presented in [19] is used and extended for state estimation for designing of robust controller for robotic manipulators.

3.1. FL+UDE controller

Consider the dynamics given by Equation (3). Because exact system model is rarely known in practice, it becomes necessary to account for the modeling errors and inaccuracies. To this end, in the

DOI: 10.1002/rnc

present work, the inertia matrix, $M(\theta)$ is taken as uncertain with $M(\theta) = M_o + \Delta M(\theta)$ where M_o is a chosen constant diagonal matrix and $\Delta M(\theta)$ is its associated uncertainty. Further, the matrices $C(\theta, \dot{\theta})$ and $K(\theta)$ are assumed to be completely unknown. In view of the considered uncertainty in $M(.)$, the dynamics of Equation (3) can be rewritten as

$$\ddot{\theta} = [-M(\theta)^{-1}C(\theta, \dot{\theta}) - M(\theta)^{-1}K(\theta) + (M(\theta)^{-1} - M_o^{-1})\tau] + M_o^{-1}\tau + d' \tag{8}$$

where d' may represent the effect of external disturbances, if any. Because $C(.)$ and $K(.)$ are assumed as completely unknown, they form a part of the total uncertainty d that needs to be estimated, and to this end, the total uncertainty d is defined as

$$d = -M(\theta)^{-1}C(\theta, \dot{\theta}) - M(\theta)^{-1}K(\theta) + (M(\theta)^{-1} - M_o^{-1})\tau + d' \tag{9}$$

In view of Equation (9), the dynamics of Equation (8) takes the form

$$\ddot{\theta} = d + M_o^{-1}\tau \tag{10}$$

where $d = [d_1\ d_2]^T$. With M_o diagonal, it is straightforward to verify that the dynamics of Equation (10) is decoupled. In view of this, the dynamics for the i-th link can be written as

$$\ddot{\theta}_i = d_i + b_{ii}\tau_i; \tag{11}$$

where b_{ii} are the diagonal elements of M_o^{-1}. To address the issue of the uncertainty, the FL control takes the form as

$$\tau_i = \frac{1}{b_{ii}}(u_{di} + \nu_i); \tag{12}$$

where u_{di} is that part of the control, which cancels the effect of uncertainties. We designate the controller of Equation (12) as FL+UDE controller. Substituting Equation (12) in Equation (11) leads to

$$\ddot{\theta}_i = u_{di} + \nu_i + d_i \tag{13}$$

From where one gets

$$d_i = \ddot{\theta}_i - u_{di} - \nu_i \tag{14}$$

In view of Equation (14) and following the procedure given in [18,19], the estimate of d_i is obtained as

$$\hat{d}_i = G_{if}(s)(\ddot{\theta}_i - u_{di} - \nu_i) \tag{15}$$

where $\hat{d}_i$ is an estimate of d_i, and $G_{if}(s)$ is a first-order low pass filter with a time constant of τ_{if}.

$$G_{if}(s) = \frac{1}{1 + \tau_{if}s}; \quad i = 1, 2 \tag{16}$$

Selecting $u_{di} = -\hat{d}_i$ and using Equation (15), one gets

$$u_{di} = -G_{if}(s)(\ddot{\theta}_i - u_{di} - \nu_i) \tag{17}$$

Now, solving for u_{di} leads to

$$u_{di} = -\hat{d}_i = -\frac{G_{if}(s)}{1 - G_{if}(s)}(\ddot{\theta}_i - \nu_i) \tag{18}$$

Substitution of Equations (6) and (18) in Equation (12) gives the FL+UDE controller. The time domain form of the resulting controller is

$$\tau_i = \frac{1}{b_{ii}}\left[-\frac{1}{\tau_{if}}\dot{\theta}_i + \nu_i + \frac{1}{\tau_{if}}\int \nu_i dt\right] \tag{19}$$

DOI: 10.1002/rnc

Clearly, under the assumption of $\hat{d}_i \approx d_i$, application of the control (19) to the dynamics of (10) results into the same error dynamics as given by Equation (7), thus eliminating the effect of uncertainties and therefore robustifying the FL controller. The robustified FL control (12) has been designated as the FL+UDE controller. Whereas the controller achieves the objective of robustification of the FL control, the implementation of the same requires measurement of joint positions as well as velocities as is obvious from Equation (19). The estimation of velocities are obtained by UDE-based observer as presented in the next section.

4. UNCERTAINTY AND DISTURBANCE ESTIMATION BASED CONTROLLER–OBSERVER STRUCTURE

The FL+UDE controller (12) or alternatively (19) requires link velocity measurement apart from the link positions for its implementation. As a solution to this problem, a design of UDE-based robust observer is proposed in this section.

4.1. Uncertainty and disturbance estimation based observer

As is obvious from Equation (11), the dynamics are decoupled, and hence observer design for i-th link only is presented. To this end, defining $x_{i1} = \theta_i$ and $x_{i2} = \dot{\theta}_i$, the dynamics of Equation (11) can be rewritten in a phase variable state-space model form as

$$\begin{aligned} \dot{x}_{i1} &= x_{i2} \\ \dot{x}_{i2} &= b_{ii}\tau_i + d_i \\ y_i &= x_{i1} \end{aligned} \tag{20}$$

Defining the state vector as $x_{ip} = [x_{i1}\ x_{i2}]^T = [\theta_i\ \dot{\theta}_i]^T$, the system of (20) can be written as

$$\begin{aligned} \dot{x}_{ip} &= A_{ip}x_p + B_{ip}\tau_i + B_{id}d_i \\ y_{ip} &= C_{ip}x_{ip} \end{aligned} \tag{21}$$

where

$$A_{ip} = \begin{bmatrix} 0 & 1 \\ 0 & 0 \end{bmatrix};\ B_{ip} = \begin{bmatrix} 0 \\ b_{ii} \end{bmatrix};\ B_{id} = \begin{bmatrix} 0 \\ 1 \end{bmatrix};\ C_{ip} = [1\ \ 0]$$

It may be noted that a conventional Luenberger observer will not be able to provide accurate state estimation for the plant of Equation (21), owing to the presence of the uncertainty. In view of this, a Luenberger-like observer of the following form is proposed as

$$\begin{aligned} \dot{\hat{x}}_{ip} &= A_{ip}\hat{x}_{ip} + B_{ip}\tau_i + B_{id}\hat{d}_i + L_i(y_{ip} - \hat{y}_{ip}) \\ \hat{y}_{ip} &= C_{ip}\hat{x}_{ip} \end{aligned} \tag{22}$$

where $L_i = [\beta_{i1}\ \beta_{i2}]^T$ is the observer gain vector. The observer however requires estimate of the uncertainty, that is, $\hat{d}_i$. Because the uncertainty is the same as present in Equation (11), the UDE-estimated uncertainty is used in the observer (22) too, giving rise to the UDE-based controller–observer structure. It may be noted that the proposed observer does not need an accurate plant model and is robust. Noting that $\hat{x}_{ip} = [\hat{x}_{i1}\ \hat{x}_{i2}]^T = [\hat{\theta}_i\ \hat{\dot{\theta}}_i]^T$, the FL+UDE control of (12) with v_i of Equation (6) and u_{di} of Equation (18), both evaluated using the UDE observer estimated states given by Equation (22), the issue of requirement of link velocity measurement is addressed.

5. CLOSED-LOOP STABILITY

The FL+UDE control (12) using v_i of Equation (6) evaluated using the observer estimated states and using $u_{di} = -\hat{d}_i$ can be written as

$$\tau_i = \frac{1}{b_{ii}}\left[\ddot{\theta}_i^\star + k_{i1}(\theta_i^\star - \hat{\theta}_i) + k_{i2}(\dot{\theta}_i^\star - \hat{\dot{\theta}}_i) - \hat{d}_i\right] \tag{23}$$

DOI: 10.1002/rnc

Denoting the reference state vector $R_i = [\theta_i^\star \ \dot{\theta}_i^\star]^T$ and defining the state feedback gain vector, K_{ip} as $K_{ip} = [m_{i1} \ m_{i2}]$ with the elements as $m_{i1} = \frac{k_{i1}}{b_{ii}}$, $m_{i2} = \frac{k_{i2}}{b_{ii}}$, the controller (23) is rewritten as

$$\tau_i = -K_{ip}\hat{x}_{ip} + K_{ip}R_i - \frac{1}{b_{ii}}\hat{d}_i + \frac{1}{b_{ii}}\ddot{\theta}_i^\star \tag{24}$$

It is straightforward to show that the dynamics of reference state vector, R_i, can be written as

$$\dot{R}_i = A_{ip}R_i + B_{id}\ddot{\theta}_i^\star \tag{25}$$

Defining the state tracking error, $e_{ic} = R_i - x_{ip}$ and using Equations (21), (24), and (25), and carrying out some simplifications lead to the following state tracking error dynamics

$$\dot{e}_{ic} = (A_{ip} - B_{ip}K_{ip})e_{ic} - (B_{ip}K_{ip})e_{io} - B_{id}\tilde{d}_i \tag{26}$$

where $\tilde{d}_i = d_i - \hat{d}_i$ is the uncertainty estimation error, and $e_{io} = x_{ip} - \hat{x}_{ip}$ is the observer state estimation error vector.

Next, the observer error dynamics can be obtained by subtracting Equation (22) from Equation (21) as

$$\dot{e}_{io} = (A_{ip} - L_iC_{ip})e_{io} + B_{id}\tilde{d}_i \tag{27}$$

Lastly, the uncertainty estimation error dynamics is obtained. From Equations (14) and (15), the estimate of the uncertainty, d_i, is given as

$$\hat{d}_i = G_{if}(s)d_i \tag{28}$$

From Equation (28), one has

$$d_i = \frac{\hat{d}_i}{G_{if}(s)} \tag{29}$$

With the uncertainty estimation error defined as $\tilde{d}_i = d_i - \hat{d}_i$ and using Equation (16) and carrying out some simplifications give

$$\dot{\tilde{d}}_i = -\frac{1}{\tau_{if}}\tilde{d}_i + \dot{d}_i \tag{30}$$

Combining Equations (26), (27), and (30) yields the following error dynamics for the controller–observer combination

$$\begin{bmatrix} \dot{e}_{ic} \\ \dot{e}_{io} \\ \dot{\tilde{d}} \end{bmatrix} = \begin{bmatrix} (A_{ip} - B_{ip}K_{ip}) & -(B_{ip}K_{ip}) & -B_{id} \\ 0 & (A_{ip} - L_iC_{ip}) & B_{id} \\ 0 & 0 & -\frac{1}{\tau_{if}} \end{bmatrix} \begin{bmatrix} e_{ic} \\ e_{io} \\ \tilde{d}_i \end{bmatrix} + \begin{bmatrix} 0 \\ 0 \\ 1 \end{bmatrix} \dot{d}_i \tag{31}$$

From Equation (31), the system matrix being in a block triangular form, it can be easily verified that the eigenvalues of the system matrix are given by

$$|sI - (A_{ip} - B_{ip}K_{ip})||sI - (A_{ip} - L_iC_{ip})||s - (-\frac{1}{\tau_{if}})| = 0 \tag{32}$$

Noting that the pair (A_{ip}, B_{ip}) is controllable, and the pair (A_{ip}, C_{ip}) is observable, the controller gain, K_{ip}, and the observer gain, L_i, can be chosen appropriately along with $\tau_{if} > 0$ to ensure stability for the error dynamics. As the error dynamics is driven by $\dot{d}_i$, it is obvious that, for bounded $|\dot{d}_i|$, bounded input-bounded output stability is assured. Finally, if the rate of change of uncertainty is negligible, that is, if $\dot{d}_i \approx 0$, then the error dynamics is asymptotically stable.

As has been stated, the error dynamics (31) is asymptotically stable if $\dot{d}_i \approx 0$. However, asymptotic stability for the error dynamics can always be assured if some higher derivative of

DOI: 10.1002/rnc

the uncertainty is equal to zero. For example, if $\dot{d}_i \neq 0$ but some higher derivative of d_i is zero, then the asymptotic stability of the error dynamics can be guaranteed by choosing an appropriate higher-order filter [19] in place of the one chosen in Equation (16).

As stated in Section 3.1, the u_{di} is that part of control, which cancels the effect of uncertainties. It is important to address the issue of existence of such a control. Although a detailed study on the existence of u_{di} is not attempted here, some comments can be offered. The control u_{di} is derived under the assumption that some derivative of d_i is negligibly small, that is, any d_i that can be approximated by functions of the type $a_o + a_1 t + a_2 t^2 + ...$ where a_i, $i = 1, 2, \ldots$ are unknown constants. The control, u_{di}, does not exist for systems in which d_i, $\dot{d}_i$ and so on are discontinuous. For systems where the derivatives of d_i are finite and small, instead of asymptotic stability, one may get uniform ultimate boundedness. This facilitates the design of u_{di} in many practical situations. Now some comments on the choice of the filter time constant are in order. From Equations (29)–(30), it can be observed that the choice of the filter time constant, τ_{if}, affects the uncertainty estimation error accuracy, that is, the uncertainty estimation error, $\tilde{d}_i$, is proportional to τ_{if} implying that smaller value of the filter constant leads to a smaller estimation error. It can also be noted that estimation does not depend on the magnitude of the uncertainty as such, but does depend on its rate of change. Further, one can note that the filter time constant acts as the time constant of the uncertainty estimation error dynamics, meaning that smaller value of the filter constant leads to faster uncertainty estimation convergence. From control efforts' point of view, the magnitude of the control increases with $1/\tau_{if}$ as is evident from Equation (19). Thus, the choice of the filter constant is a tradeoff between estimation accuracy and its rate of convergence on the one hand, and the control efforts on the other hand.

6. SIMULATIONS AND RESULTS

In this section, numerical simulation results using the FL+UDE controller of (12) with v_i of Equation (6) and u_{di} of Equation (18), both evaluated using the UDE observer estimated states given by Equation (22) are presented. The link parameters used in the simulations, as taken from [34], are given in Table I. In simulations, the tracking specification for each link is considered in terms of the desired settling time and damping ratio as given in Table I. Consequently, the controller gains k_{i1} and k_{i2} required in Equation (6) are chosen to satisfy these specifications. The observer gains, β_{ij}'s are obtained by placing the observer poles at -300 for both the links. The initial conditions for the observer as well as for the plant variables are taken as zero. In simulations, uncertainty is introduced by considering m_1 and m_2 uncertain by -50% of their respective nominal values. Further, a load disturbance torque of -30% of maximum input torques is considered. The desired position trajectory is taken as $\theta_1^\star = 30\sin(t)$ deg and $\theta_2^\star = -30\sin(t)$ deg. The values of b_{ii} are taken as inverse of the diagonal elements of the inertia matrix given in Equation (2) with cosine term approximated to unity. Actuator saturation limits of $\tau_{1max} = \pm 50$ N-m and $\tau_{2max} = \pm 10$ N-m have been considered in the simulations. With these data, simulations are carried out, and the results are presented in Figure 2. In Figures 2(a)–(b), the reference, estimated and actual joint positions are plotted, and it can be seen that the observer estimates the states accurately. Also, from time history

Table I. Simulation parameters.

Parameter	Definition	Value
m_1	Mass of link 1	2 kg
m_2	Mass of link 2	1 kg
l_1	Length of link 1	2 m
l_2	Length of link 2	1 m
g	Gravitational acceleration	9.8 m/s^2
t_{s_1}, t_{s_2}	Desired settling times	0.5 s
ζ_1, ζ_2	Damping ratios	1
τ_{1f}, τ_{2f}	Filter time constants	0.05 s

DOI: 10.1002/rnc

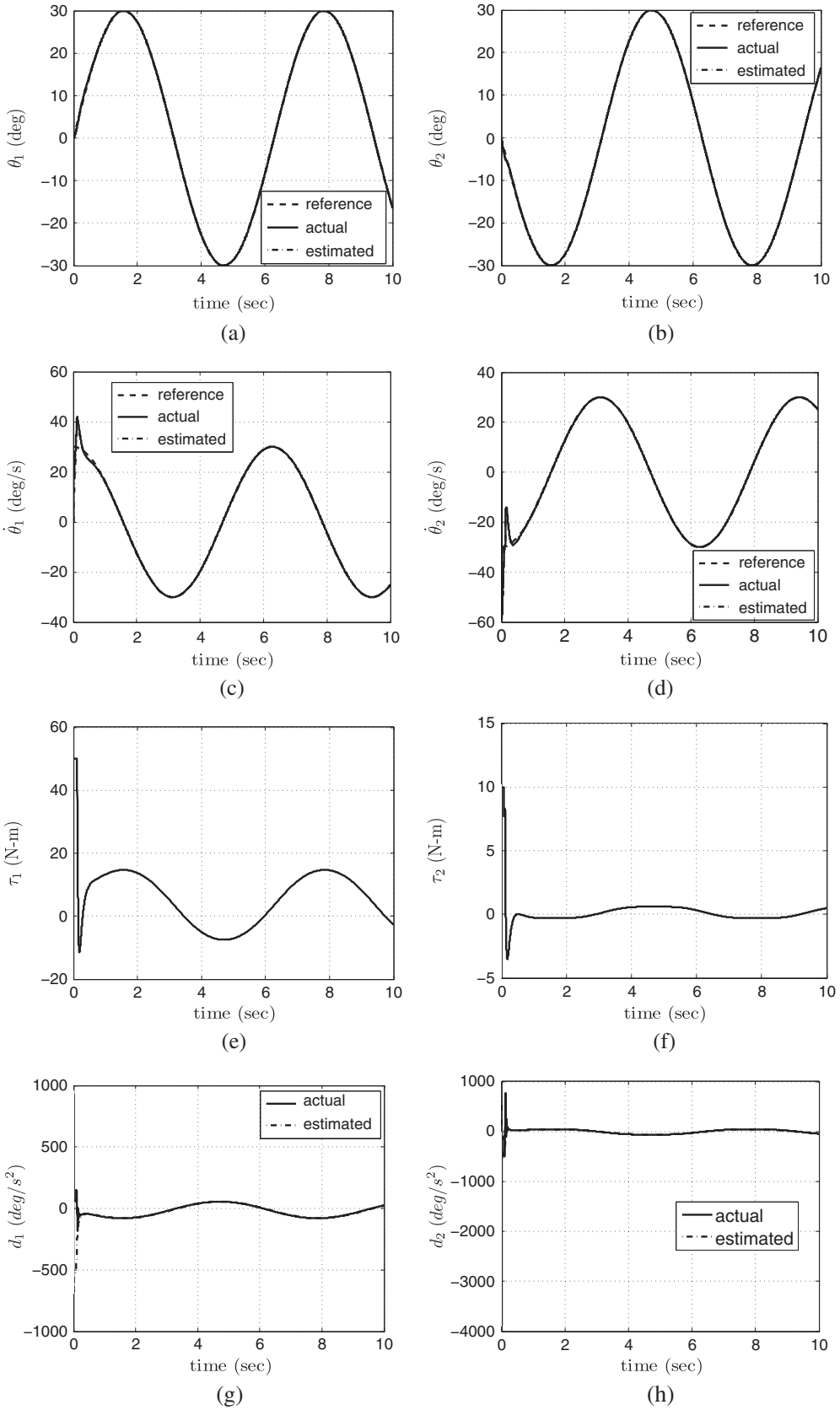

Figure 2. Performance of UDE-based controller.

DOI: 10.1002/rnc

of reference trajectory, it can be seen that the UDE-based controller–observer offered a highly satisfactory tracking performance despite the significant model uncertainty. The reference, estimated and actual link velocities are given in Figures 2(c)–(d), and one can observe that the estimation is quite satisfactory. The time histories of the actual and estimated uncertainties for both the links are given in Figures 2(g)–(h) from where it can be observed that the UDE estimator has estimated the uncertainty quite accurately. The time histories of the input torques are shown in Figures 2(e)–(f).

7. COMPARISON WITH EXISTING DESIGNS

Simulations are carried out to compare the performance of the proposed design with some well-known existing controllers. The controllers considered for comparison purpose are: (1) gravity compensated PD control; (2) FL-based control; (3) FL controller with Lyapunov-based outer-loop design; and (4) controller based on SMC theory. A brief of the controllers are as follows:

Design-1: Proportional-derivative control with gravity compensation.

A gravity-compensated PD controller [1] of the following form

$$\tau = K_p(\theta^\star - \theta) + K_d(\dot{\theta}^\star - \dot{\theta}) + \bar{K}(\theta) \tag{33}$$

where $K_P >,\ K_D > 0$ are the diagonal gain matrices, and $\bar{K}(\theta)$ is the nominal gravity matrix. It has been shown that the simple PD controller with gravity compensation offers robustness for set-point control of robot manipulators [12]. For simulations, gains K_P and K_D are chosen to satisfy the desired settling time and damping ratio given in Table I. The design is referred to as Design-1.

Design-2: Feedback linearization based control.

An FL [1]-based controller without robustification is considered as Design-2 for comparison. The control law is

$$\tau = \bar{C} + \bar{K} + \bar{M}\nu \tag{34}$$

where $\bar{M}$, $\bar{C}$, and $\bar{K}$ are the nominal values for the respective matrices, which are obtained from Equation (2) by using the parameters given in Table I. The outer-loop control, ν, is chosen as

$$\nu = \ddot{\theta}^\star + K_P(\theta^\star - \theta) + K_D(\dot{\theta}^\star - \dot{\theta}) \tag{35}$$

wherein K_P and K_D are the diagonal gain matrices chosen in similar manner as carried out in Design-1.

Design-3: Lyapunov-based control.

FL control with Lyapunov-based outer-loop design given in [1] is used as Design-3 in this comparison. Using Lyapunov's second method, the control law designed for two-link robot manipulator takes the form

$$\tau = \bar{C} + \bar{K} + \bar{M}\nu \tag{36}$$

with the outer-loop design given by

$$\nu = \ddot{\theta}^\star + K_P(\theta^\star - \theta) + K_D(\dot{\theta}^\star - \dot{\theta}) + W \tag{37}$$

where $W = [W_1\ W_2]^T$ with

$$W_i = \begin{cases} D_i \dfrac{B_i^T P_i e_i}{|B_i^T P_i e_i|} & \text{if} |B_i^T P_i e_i| \geqslant \epsilon_i \\ D_i \dfrac{B_i^T P_i e_i}{\epsilon} & \text{if} |B_i^T P_i e_i| < \epsilon_i, \quad i = 1, 2 \end{cases} \tag{38}$$

The P_i is a unique symmetric positive definite matrix satisfying the Lyapunov equation

$$A_i^T P_i + P_i A_i + I = 0 \tag{39}$$

DOI: 10.1002/rnc

and $e_i = [e_{ic}\ \dot{e}_{ic}]^T$. The quantities $D_i,\ i = 1, 2$ are the bounds on uncertainty, the values of which have been taken as $D_1 = 100$ and $D_2 = 300$ in the simulations. The nominal values $\bar{M}$, $\bar{C}$, and $\bar{K}$ are obtained by evaluating Equation (2) using the link parameters from Table I, and the controller gains K_P and K_D are found out to satisfy the desired performance specifications.

Design-4: SMC-based control.

SMC-based design, as given in [35], is used as Design-4 for the purpose of comparison. The resulting SMC for the two-link robot manipulator is

$$\tau = \tau_{eq} + \tau_n \tag{40}$$

where τ_{eq} is responsible for the performance of the nominal system and is given by

$$\tau_{eq} = \bar{C} + \bar{K} + \bar{M}v \tag{41}$$

whereas the control τ_n is that part of the control, which rejects the effect of uncertainties and disturbances. Considering the sliding surface, [35], as

$$s = \dot{q}_e + K_D q_e \tag{42}$$

where $q_e = \theta^\star - \theta$, the control, τ_n, is given by

$$\tau_n = Dsgn(s) \tag{43}$$

where D represents the assumed bound on uncertainty. To avoid chattering, a saturation function, $sat(s/\epsilon)$, is used in place of the signum function, $sgn(s)$. The saturation function is given by

$$sat(s/\epsilon) = \begin{cases} \frac{s}{||s||} & \text{if } ||s|| > \epsilon \\ \frac{s}{\epsilon} & \text{if } ||s|| \leqslant \epsilon \end{cases} \tag{44}$$

where ϵ represents width of the boundary layer. In simulations, the bound on uncertainty, D, is selected as a diagonal matrix with diagonal elements of 100 and 300, which are the same as the bounds of uncertainty considered in Design-3, and the width of the boundary layer, ϵ, is taken as 0.1. Simulation data are taken from Table I, and the controller gains K_P and K_D are found out to satisfy the desired performance specifications.

Design-5: UDE-based control.

The proposed FL+UDE based controller of (12) with v_i of Equation (6) and u_{di} of Equation (18), both evaluated using the UDE-based observer estimated states given by Equation (22) is designated as Design-5 for comparison purpose. Simulation parameters and other design parameters are the same as given in Section 6. To compare the performance, simulations are carried out by using the data given in Table I for all the designs. In simulations, uncertainty is introduced by considering m_1 and m_2 uncertain by -50% from their respective nominal values. Further, a load disturbance torque of -30% of maximum input torque is also considered, and the results are presented in Figure 3. From the figures, it can be observed that whereas the Designs 1–3 have resulted in steady state error in position and velocity tracking, the observer-based FL+UDE controller has offered better tracking performance. It can also be noted that, in the presence of load torque disturbance, the amount of input torque required for UDE-based design is less compared with the other designs. The ratio of absolute value of the maximum magnitude of tracking error to the amplitude of the reference signal for all the five designs is presented in Table II, and it can be noticed that the values of ratios for link positions for Designs 1–3 are higher compared with the UDE-based design.

From the figures, it can be observed that the tracking performance of the SMC-based approach is comparable with that of the UDE-based controller. However, as can be seen from Figure 3(f), the control input, τ_2, is significantly higher in the case of SMC in comparison with the UDE-based design. Also, one can notice from Table II that the value of the ratio for the first-link position is higher for SMC in comparison with the proposed UDE-based design.

DOI: 10.1002/rnc

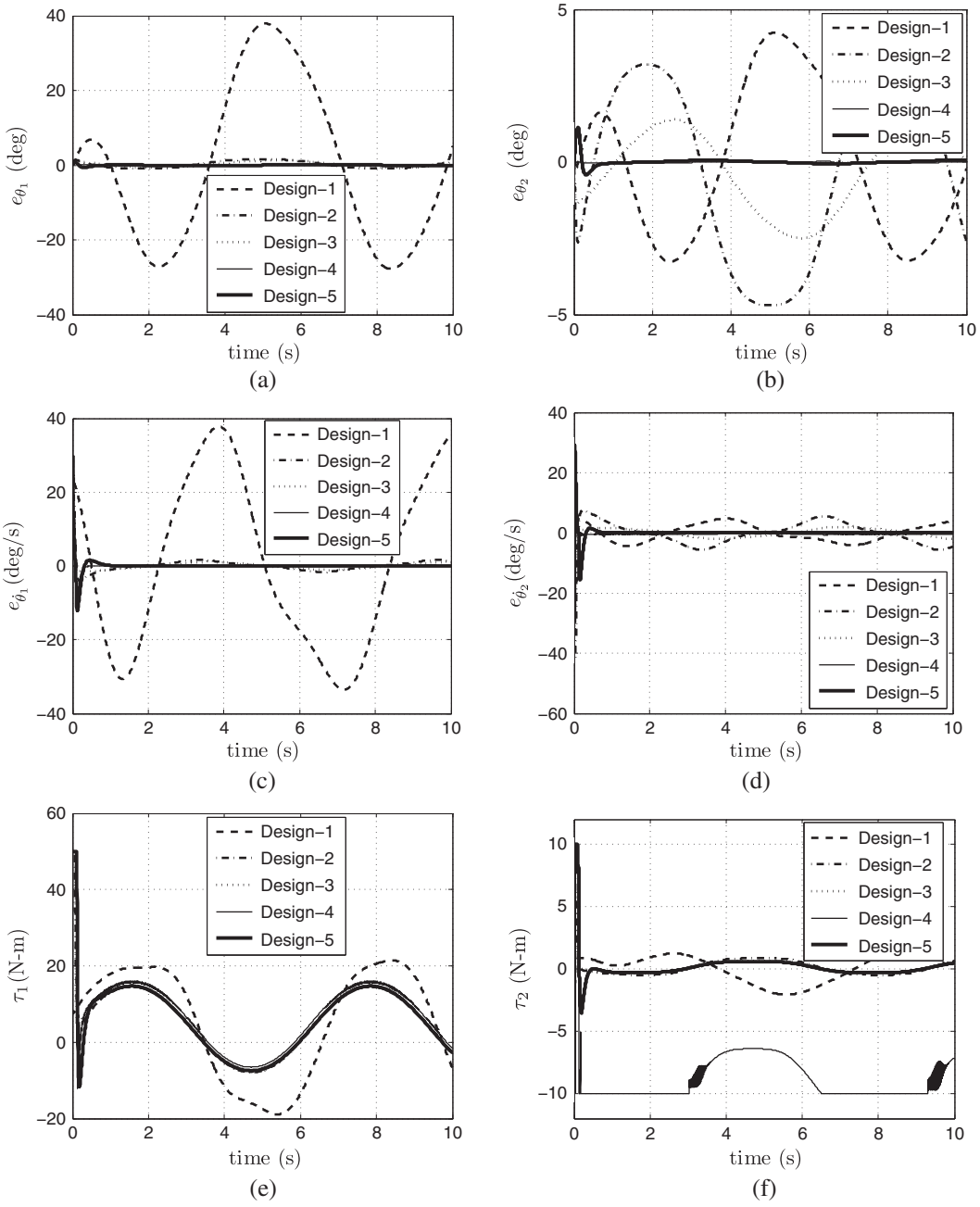

Figure 3. Performance comparison with existing designs.

Here, it is important to note that, in the simulations of Designs 1–4, true values of the joint positions and velocities are used whereas in Design 5, the UDE observer estimated values are used. Naturally, if the Designs 1–4 are simulated in conjunction with a separately designed observer, the performance is expected to degrade. It may also be noted that the Designs 1–4 use exact expressions of system matrices with nominal values of the system parameters, that is, $\bar{M}$, $\bar{C}$, and $\bar{K}$ in contrast to the proposed design wherein the system nonlinearities have been considered as a part of the uncertainties and thus assumed as unknown. The designs based on the Lyapunov and the SMC controllers need a knowledge of reasonably accurate bounds of uncertainty. It is logical that, when the controllers are implemented with inaccurate information of knowledge of bound on uncertainty,

DOI: 10.1002/rnc

Table II. Comparative performance of various design techniques.

Design	θ_1	θ_2	$\dot{\theta}_1$	$\dot{\theta}_2$
PD control with gravity compensation	1.2628	0.1416	1.2590	1.0000
Feedback linearization based control	0.0527	0.1564	1.0000	1.3863
Lyapunov-based control	0.0422	0.0833	1.0000	1.0785
Control based on sliding mode control	0.0328	0.0034	1.0000	1.0000
UDE	0.0261	0.0376	1.0000	1.0000

the performance would not be the same as the one presented here. On the other hand, the proposed UDE-based design offers certain distinct advantages. Firstly, it neither requires the knowledge of bounds of uncertainty nor exacts system model. Secondly, the controller does not need availability of all the states as the UDE technique employed for design of controller is also employed for designing a robust observer in an integrated manner. Lastly, whereas there exists a possibility of chattering in control signal in the case of SMC design, the control signal is smooth in the proposed UDE-based design. It may also be noted that, following the similar logic as that of the gravity-compensated PD control, the proposed UDE-based controller may be called as uncertainty-compensated PD control.

8. EXPERIMENTAL VALIDATION

In this work, the efficacy of the proposed UDE-based controller is demonstrated experimentally on the Quanser's rotary single-link flexible joint module. In literature, various control schemes are proposed to address the issue of joint flexibility. An SMC-based strategy is proposed in [36] wherein the design needs knowledge of the bounds of uncertainty and also the complete state vector for its implementation. In [37], a dynamic feedback controller is proposed for trajectory tracking control problem of robotic manipulators with flexible joints. The design needs position measurements on the link as well as the motor side, and the velocities required in the controller are estimated through a reduced order observer. The robustness of the closed-loop system is established by assuming that the uncertainties satisfy certain conditions. Application of the singular perturbation approach can be found in [38] wherein the controller needs measurements of position and elastic force. A nonlinear sliding state observer is used for estimating the link velocities and elastic force time derivatives. Controller design based on adaptive control [39], back-stepping approach [40], and integral manifold formulation [41] are some other approaches reported in the literature. Most of the schemes that appeared in the literature have certain issues that require attention. Firstly, many of them require measurements of all state variables or at least the position variables on link and motor side. Next, robustness wherever guaranteed, is often highly model dependent. Also, in some approaches, knowledge of some characteristics of the uncertainties such as its bounds is required. Because of highly nonlinear dynamics, the FL approach has also been proposed for designing the trajectory tracking controllers for flexible joint robots [1, 36, 41]. As stated earlier, the FL offers asymptotic tracking of the reference trajectory only when the model is known exactly, and the fed back states are measured without any error. Another important consideration is that the FL control needs complete state vector for its implementation. In contrast, the UDE-based design proposed in this work does not need exact model and is robust as the system uncertainties are estimated and compensated. The design does not need any information about the uncertainties, such as its bound. Further, by using the UDE-based observer, the proposed design requires measurement of position only for its implementation.

The Quanser's rotary single-link flexible joint experimental setup consists of Quanser UPM 1503 module, Quanser Q4 data acquisition and control board, Quanser SRVO2 plant, Quanser rotary flexible joint module, and a PC equipped with necessary softwares including the Quanser WinCon. The Q4 is a hardware-in-loop data acquisition and control board with extensive range of input and output support. The UPM-1503 is a power amplifier that drives the motor. The WinCon software provides hardware-in-the-loop simulation environment, that is, a Simulink-based user-designed controller that can be run in real-time using the WinCon environment. The rotary single-link flexible joint

DOI: 10.1002/rnc

module consists of a rigid beam mounted on a flexible joint that rotates via a DC motor. The motor load angle and joint deflection are measured using optical encoders. Here, the objective is to design a feedback controller such that the tip of the beam tracks a desired command while minimizing joint deflection and resonance in the system. The experimental setup used to validate the controller is shown in Figure 4, and more details about the same can be found in [42, 43].

8.1. Mathematical model

In the Quanser's flexible joint module, a rigid link is mounted on a flexible joint that rotates via a DC servo motor. The motor load angle and joint deflection are measured using optical encoders. As the Quanser's module operates in a horizontal plane, its mathematical model differs from the one given in Equation (3). The difference is caused by the absence of gravity in the former case. The mathematical model for the Quanser's module, as given in [43], is

$$\begin{aligned} \ddot{\theta} + \frac{F_1}{J_{eq}}\dot{\theta} - \frac{K_{stiff}}{J_{eq}}\alpha &= \frac{F_2}{J_{eq}}V_m \\ \ddot{\alpha} - \frac{F_1}{J_{eq}}\dot{\theta} + \frac{K_{stiff}(J_{eq}+J_{arm})}{J_{eq}J_{arm}}\alpha &= -\frac{F_2}{J_{eq}}V_m \end{aligned} \tag{45}$$

where $F_1 \triangleq \dfrac{\eta_m \eta_g K_t K_m {K_g}^2 + B_{eq} R_m}{R_m}$ and $F_2 \triangleq \dfrac{\eta_m \eta_g K_t K_g}{R_m}$

The quantities appearing in these expressions are: θ is the motor load angle, α is the link joint deflection, η_m is the motor efficiency, η_g is the gearbox efficiency, K_t is the motor torque constant, K_m is the back EMF constant, K_g is the gearbox ratio, B_{eq} is the viscous damping coefficient, R_m is the armature resistance, J_{eq} is the gear inertia, K_{stiff} is the spring stiffness, J_{arm} is the link inertia, and V_m is the motor control voltage. The aim is to design a controller that will place the tip of link ($y = \theta + \alpha$) as desired, with minimum link deflection α. Now, taking $y = \theta + \alpha$ as link position, the dynamics in terms of y and θ is rewritten as

$$\begin{aligned} J_{arm}\ddot{y} &= -K_{stiff}(y-\theta) \\ J_{eq}\ddot{\theta} &= K_{stiff}(y-\theta) - F_1\dot{\theta} + F_2 V_m \end{aligned} \tag{46}$$

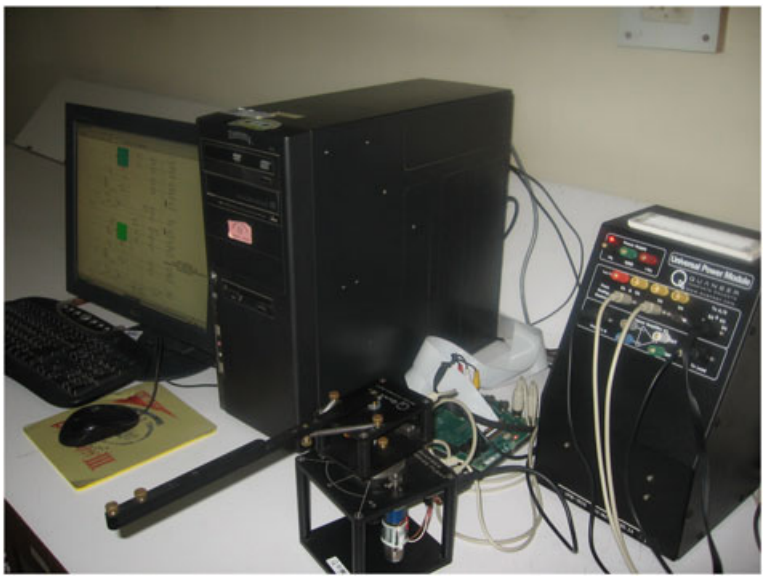

Figure 4. Quanser rigid link manipulator with flexible joint-experimental setup.

DOI: 10.1002/rnc

The related rigid model as obtained in the limit of $K \to \infty$ is [1]

$$\ddot{\theta} = -\frac{F_1}{J'}\dot{\theta} + \frac{F_2}{J'}V_m \tag{47}$$

where $J' = J_{arm} + J_{eq}$. The dynamics of Equation (47) can be written as

$$\ddot{\theta} = d + b_0 V_m \tag{48}$$

where $d = -\frac{F_1}{J'}\dot{\theta}$ and $b_0 = \frac{F_2}{J'}$.

For the dynamics of (48), the controller and the observer design is then carried out in a similar manner as outlined in Sections 3 and 4 with $u_d = -\hat{d}$, and ν defined as,

$$\nu = \ddot{\theta}^\star + k_2(\dot{\theta}^\star - \dot{\hat{\theta}}) + k_1(\theta^\star - \hat{\theta}) \tag{49}$$

The resulting controller using the observer estimated states is obtained as

$$V_m = \frac{1}{b_o}(u_d + \nu) = \frac{1}{b_o}\left(-\frac{\dot{\hat{\theta}}}{\tau_f} + \frac{1+\tau_f s}{\tau_f s}\nu\right) \tag{50}$$

or alternatively, written in time domain, the controller is given by

$$V_m = \frac{1}{b_o}\left[-\frac{1}{\tau_f}\dot{\hat{\theta}} + \nu + \frac{1}{\tau_f}\int \nu dt\right] \tag{51}$$

8.2. Experimental results

To evaluate the performance of the UDE-based FL controller, experiments are carried out on the Quanser's single-link flexible joint module. The nominal values of the various link parameters as taken from [43] are: $K_{stiff} = 1.248\,N - m/rad$, $\eta_m = 0.69$, $\eta_g = 0.9$, $K_t = 0.00767\,N - m$, $K_g = 70$, $J_{eq} = 0.00258\,kg - m^2$, $J_{arm} = 0.00352\,kg - m^2$, $R_m = 2.6\,\Omega$. The controller gains k_is are obtained by placing the poles at $\left(s + \frac{2}{\tau_c}\right)^2 = 0$ with $\tau_c = 0.2\,s$. The observer gains, β_is are obtained by placing the poles at $\left(s + \frac{2}{\tau_o}\right)^2 = 0$ with $\tau_o = \frac{\tau_c}{3}$. Note that the observer time constant is 1/3 that of the controller time constant. The initial conditions for plant as well as observer are taken as zero. The value of the time constant of the filter of Equation (16) is taken as $0.05\,s$. The desired trajectory to be tracked is taken as $30\sin(t)$ deg. The control signal generated is applied to the module through Quanser's interfacing hardware board. The experimental results are shown in Figure 5. In Figure 5(a), the tracking performance is presented from where one can observe that the link has tracked the reference quite accurately. The control input history is presented in Figure 5(b). The estimated uncertainty is given in Figure 5(c). It may also be noted that the effect of measurement noise is visible in the estimated uncertainty and so in the control signal, and the proposed design has offered satisfactory performance notwithstanding the noisy measurement.

The experimental results presented in Figure 5 are for reference trajectory of $30\sin(t)$ deg corresponding to the time period of 2π s. To ascertain the performance of the controller when the input is fast-varying, experiments are carried out using the proposed UDE-based controller with a reference trajectory of a time period of 2 s, and the results are presented in Figure 6. From the figures, it can be observed that the tracking performance has deteriorated. The deterioration in the performance is caused by the increased inaccuracy in the uncertainty estimation. As is evident from Equation (30), the uncertainty estimation error dynamics is driven by the rate of change of uncertainty, that is, $\dot{d}$. If the uncertainty is fast-varying, the resulting estimation accuracy may degrade. In the present case, as the frequency of the input signal is increased, the resulting state-dependent uncertainty, d, as defined in Equation (48) is also fast-varying, thereby resulting into the degraded uncertainty estimation and so in the tracking performance.

DOI: 10.1002/rnc

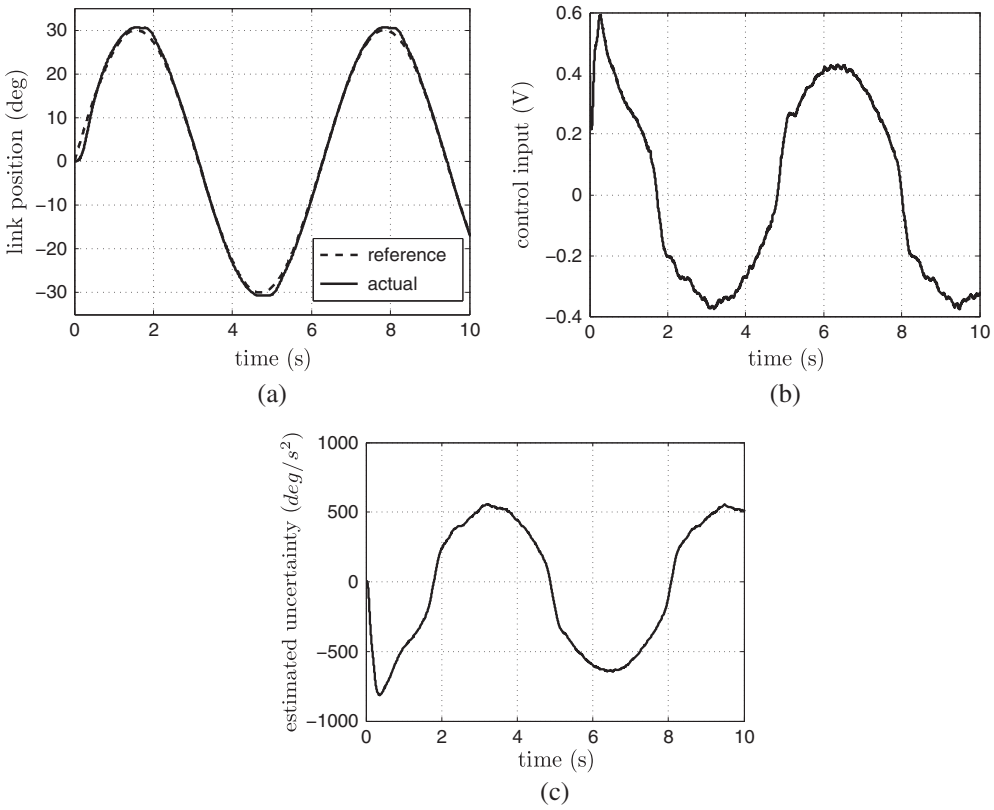

Figure 5. Experimental tracking performance.

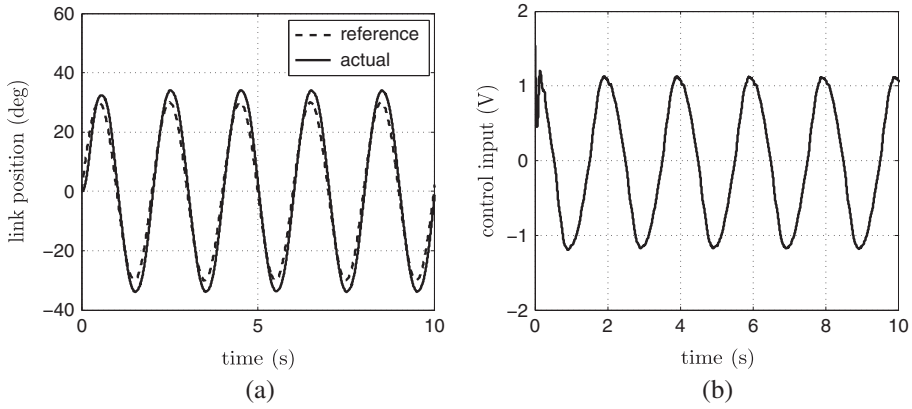

Figure 6. Experimental tracking performance with first-order filter: Ref. trajectory of 2-s time period.

One approach in tackling fast-varying uncertainty in the UDE approach is to design an appropriate filter instead of the first-order filter given in Equation (16). For example, if a second-order filter [19] of the form

$$G_f(s) = \frac{(1+\tau_f s)^2 - (\tau_f s)^2}{(1+\tau_f s)^2} \tag{52}$$

is used, the resulting UDE-based controller using the UDE observer estimated states can be obtained as

DOI: 10.1002/rnc

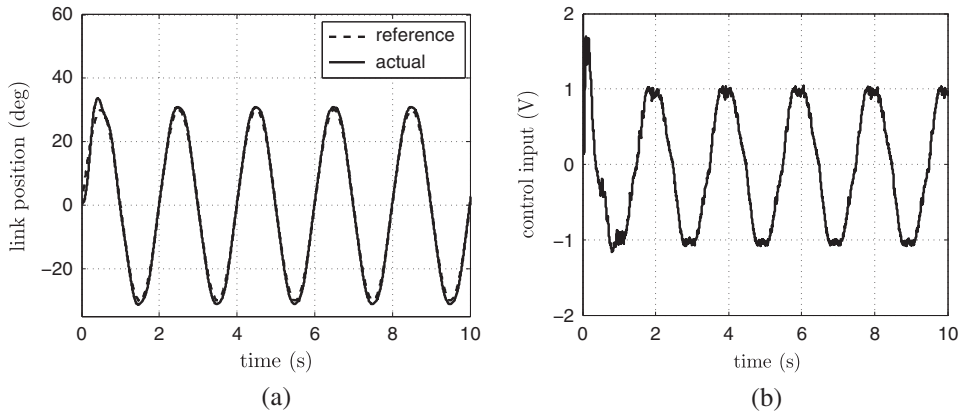

(a) (b)

Figure 7. Experimental tracking performance with second-order filter: Ref. trajectory of 2-s time period.

$$V_m = \frac{1}{b_o}\left[-\frac{2}{\tau_f}\left(\dot{\hat{\theta}} - \int \nu dt\right) - \frac{1}{\tau_f^2}\left(\hat{\theta} - \int\left(\int \nu dt\right) dt\right) + \nu\right] \tag{53}$$

In implementation of the controller (53), the value of filter time constant is chosen as 0.1 s, and the controller and observer gains are obtained by taking $\tau_c = 0.1$ and $\tau_o = \tau_c/3$. Using these controller parameters, experiments are carried out for the sinusoid input of a time period of 2 s, and the results are shown in Figure 7. By comparison of the results of Figures 6 and 7, it can be observed that the use of the second-order filter has resulted in better tracking performance.

9. CONCLUSIONS

In this paper, a new approach based on the UDE technique is proposed for designing a robust trajectory tracking controller for robot manipulators. The feedback linearizing controller designed is robustified by augmenting it with the UDE-estimated uncertainties. In doing so, the system nonlinearities, external disturbances, and modeling inaccuracies have been considered as the part of the estimated uncertainty. As the controller thus designed needs joint velocity measurements, the same are obtained by designing a robust observer, which too employs the UDE-estimated uncertainties to achieve robustness. The notable features of the proposed strategy is that it does not need knowledge of any characteristic of the uncertainty. Also, the design does not require accurate plant model. Closed-loop stability of the overall system is established. Numerical simulation results of application of the proposed strategy to trajectory tracking control of two-link robot manipulator are presented, and it is shown that the proposed strategy offers desired performance notwithstanding significant model uncertainties. Performance comparison of the proposed strategy with some well-known controllers shows that the proposed design offers better robustness and performance. Lastly, efficacy of the proposed approach is established through experimental validation as applied to the Quanser's single-link flexible joint module.

REFERENCES

1. Spong MW, Vidyasagar M. *Robot Dynamics and Control*. Wiley: New York, 1989.
2. Dawson DM, Qu Z, Lewis FL, Dorsey JF. Robust control for the tracking of robot motion. *International Journal of Control* 1990; **52**(3):581–595.
3. Alvarez-Ramirez J, Cervantes I, Kelly R. PID regulation of robot manipulators: stability and performance. *Systems and Control Letters* 2000; **41**(2):73–83.
4. Stout WL, Sawan ME. Application of H-infinity theory to robot manipulator control. *Proceedings of the IEEE Conference on Control Applications*, Dayton, OH, USA, 13–16 September 1992; 148–153.
5. Spong MW. On the robust control of robot manipulators. *IEEE Transactions on Automatic Control* 1992; **37**(11):1782–1786.

DOI: 10.1002/rnc

6. Stepanenko Y, Cao Y, Su C-Y. Variable structure control of robotic manipulator with PID sliding surfaces. *International Journal of Robust and Nonlinear Control* 1998; **8**(1):79–90.
7. Lin F, Brandt RD. An optimal control approach to robust control of robot manipulators. *IEEE Transactions on Robotics and Automation* 1998; **14**(1):69–77.
8. Xin M, Balakrishnan SN, Huang Z. Robust state dependent Riccati equation based robot manipulator control. *Proceedings of the IEEE International Conference on Control Applications*, Mexico City, Mexico, 2001; 369–374.
9. Lewis FL. Neural network control of robot manipulators. *IEEE Expert Magazine* 1996; **11**(3):64–75.
10. Ham C, Qu Z, Johnson R. Robust fuzzy control for robot manipulators. *IEE Proceedings - Control Theory and Applications* 2000; **147**(2):212–216.
11. Abdallah C, Dawson D, Dorato P, Jamshidi M. Survey of robust control for rigid robots. *IEEE Control Systems Magazine* 1991; **11**(2):24–30.
12. Sage HG, Mathelin MFD, Ostertag E. Robust control of robot manipulators: a survey. *International Journal of Control* 1999; **72**(16):1498–1522.
13. You SS, Hall JL. Robust motion tracking controllers for uncertain robot manipulators. *Proceedings of the Institution of Mechanical Engineers, Part I: Journal of Systems and Control Engineering* 1995; **209**(14):269–280.
14. Spong MW, Thorp JS, Kleinwaks JM. Robust microprocessor control of robot manipulators. *Automatica* 1987; **23**(3):373–379.
15. Zhao D, Li S, Zhu Q, Gao F. Robust finite-time control approach for robotic manipulators. *IET Control Theory and Applications* 2010; **4**(1):1–15.
16. Bona B, Indri M. Analysis and implementation of observers for robotic manipulators. *Proceedings of the IEEE International Conference on Robotics and Automation*, Leuven, Belgium, 1998; 3006–3011.
17. Nicosia S, Tomei P. Robot control by using only joint position measurements. *IEEE Transactions on Automatic Control* 1990; **35**(9):1058–1061.
18. Zhong QC, Rees D. Control of uncertain LTI systems based on an uncertainty and disturbance estimator. *Transactions of the ASME, Journal of Dynamic Systems, Measurement, and Control* 2004; **126**(4):905–910.
19. Talole SE, Phadke SB. Robust input–output linearisation using uncertainty and disturbance estimation. *International Journal of Control* 2009; **82**(10):1794–1803.
20. Nijmeijer H, Schaft AVD. *Nonlinear Dynamical Control Systems*. Springer-Verlag: New York, 1990.
21. Slotine JJE, Li W. *Applied Nonlinear Control*. Prentice-Hall: Englewood Cliffs, New Jersey, 1991.
22. Chen WH. Nonlinear disturbance observer-enhanced dynamic inversion control of missile. *Journal of Guidance, Control, and Dynamics* 2003; **26**(1):161–166.
23. Takahashi RHC, Peres PLD. Unknown input observers for uncertain systems: a unifying approach and enhancements. *Proceedings of the 35th Conference on Decision and Control*, Kobe, Japan, 11–13 December 1996; 1483–1488.
24. Moura JT, Elmali H, Olgac N. Sliding mode control with sliding perturbation observer. *Transactions of the ASME, Journal of Dynamic Systems, Measurement, and Control* 1997; **119**(4):657–665.
25. Chen WH, Ballance DJ, Gawthrop PJ, O'Reilly J. A nonlinear disturbance observer for robotic manipulators. *IEEE Transactions on Industrial Electronics* 2000; **47**(4):932–938.
26. Hori Y. High performance control of robot manipulator without using inverse dynamics. *Control Engineering Practice* 1993; **1**(3):529–538.
27. Youcef-Toumi K, Ito O. A time delay controller for systems with unknown dynamics. *Transactions of the ASME, Journal of Dynamic Systems, Measurement, and Control* 1990; **112**(1):133–142.
28. Youcef-Toumi K, Shortlidge CC. Control of robot manipulators using time delay. *Proceedings of IEEE International Conference on Robotics and Automation*, Sacramento, California, USA, 9–11 April 1991; 2391–2398.
29. Chang PH, Kim DS, Park KC. Robust force/position control of a robot manipulator using time delay control. *Control Engineering Practice* 1995; **3**(9):1255–1264.
30. Patel A, Neelgund R, Wathore A, Kolhe JP, Kuber MM, Talole SE. Robust control of flexible joint robot manipulator. *Proceedings of the IEEE International Conference on Industrial Technology (ICIT 2006)*, IIT Bombay, Mumbai, India, December 2006; 649–653.
31. Talole SE, Phadke SB. Model following sliding mode control based on uncertainty and disturbance estimator. *Transactions of the ASME, Journal of Dynamic Systems, Measurement, and Control* 2008; **130**(3):034501–1–5.
32. Kuperman A, Zhong QC. Control of uncertain linear systems with a state delay based on an uncertainty and disturbance estimator. *Proceedings of the Sixth IFAC Symposium on Robust Control Design*, Haifa, Israel, 2009; 279–283.
33. Kuperman A, Zhong QC. Robust control of uncertain nonlinear systems with state delays based on an uncertainty and disturbance estimator. *International Journal of Robust and Nonlinear Control* 2011; **21**(1):79–92.
34. Bailey E, Arapostathis A. Simple sliding mode control scheme applied to robot manipulators. *International Journal of Control* 1987; **45**(4):1197–1209.
35. Shi J, Liu H, Bajcinca N. Robust control of robotic manipulators based on integral sliding mode. *International Journal of Control* 2008; **81**(10):1537–1548.
36. Spurgeon SK, Yao L, Lu XY. Robust tracking via sliding mode control for elastic joint manipulators. *Proc. Institution of Mechanical Engineers-Part I, Journal of Systems and Control Engineering* 2001; **215**(4):405–417.
37. Chang YC, Chen BS, Lee TC. Tracking control of flexible joint manipulators using only position measurements. *International Journal of Control* 1996; **64**(4):567–593.

DOI: 10.1002/rnc

38. Fernandez J, Barbot JP. Sliding observer-based feedback control for flexible joints manipulator. *Automatica* 1996; **32**(9):1243–1254.
39. Ghorbel F, Hung JY, Spong MW. Adaptive control of flexible-joint manipulators. *IEEE Control Systems Magazine* 1989; **9**(7):9–13.
40. Oh JH, Lee JS. Control of flexible joint robot system by backstepping design approach. *Proceedings of the IEEE International Conference on Robotics and Automation*, Albuquerque, New Mexico, 20–25 April 1997; 3435–3440.
41. Spong MW. Modeling and control of elastic joint robots. *Transactions of the ASME, Journal of Dynamic Systems, Measurement, and Control* 1987; **109**(4):310–319.
42. Quanser Inc. Introduction to WinCon & SRV02, Quanser Inc, Canada, 2008.
43. Quanser Inc. Rotary Flexible Joint-User Manual, Quanser Inc, Canada, 2008.

DOI: 10.1002/rnc